

# Modeling and Design of a Disk-Type Furrow Opener's Coulter Its Mechanical Analysis and Study for No-Till Machinery (Combination and Bertini)

**J. Ghezavati, M. Abbasgholipour \*, B. Mohammadi Alasti**

Department of Biosystems Mechanical Engineering,  
Bonab Branch, Islamic Azad University, Bonab, Iran  
E-mail: Ghezavati905@gmail.com, M.a\_pour@yahoo.com,  
behzad.alasti@gmail.com

\*Corresponding author

**A. Shirneshan**

Department of Mechanical Engineering, Najafabad Branch, Islamic Azad University, Najafabad, Iran  
Modern Manufacturing Technologies Research Center, Najafabad Branch, Islamic Azad University, Najafabad, Iran  
E-mail: arshirneshan@yahoo.com

**A. Shadkam**

Department of Mechanical Engineering,  
Faculty of Engineering, Bonab Branch, Islamic Azad University, Bonab, Iran

**Received: 4 June 2017, Revised: 26 June 2017, Accepted: 20 September 2017**

**Abstract:** No-till practices play an important role in decreasing production costs, increasing soil organic matter content, improving soil structure and removing unwanted environmental impacts. However, due to a lack of access to proper machinery for direct seeding in unplowed lands, such practices have failed to produce successful results since they are incapable of providing sufficient contact between soil and seeds. Introducing a machine that can plant seeds and fertilizer at two different depths in hard (unplowed) soils covered with last season's crop residues can be the first step towards pilot no-till initiatives. This step can finally lead to the promotion of this practice in the potential areas. In this study, different components of a disk furrow opener were optimally designed in Solid Works modelling software. ANSYS was used to analyze this furrow opener and its three main related components. Finally, the coulter's stress was determined using the von Mises criterion. The result showed that the minimum coulter stress was 1985.5Pa throughout the plane and its maximum belonged to the holes inside the hub with 1.0819x107Pa. The safety factor of the initial coulter was 17.85, while that of the optimally designed coulter was 25.

**Keywords:** ANSYS, Direct planting, No-till farming, Rotary coulter, Solid Works

**Reference:** Ghezavati, J., Abbasgholipour, M., Mohammadi Alasti, B., Shirneshan, A., Shadkam, A., "Modeling and Design of a Disk-Type Furrow Opener's Coulter Its Mechanical Analysis and Study for No-Till Machinery (Combination and Bertini)", Int J of Advanced Design and Manufacturing Technology, Vol. 10/No. 4, 2017, pp. 63–73.

**Biographical notes:** **J. Ghezavati** is currently a PhD student in Mechanical Engineering at Bonab Branch, Islamic Azad University, Iran. His field of research is Design and construction of Machine, Mechatronics, Post-harvest, Nano Materials and Composite Materials. **M. Abbasgholipour** obtained his PhD in Mechanical Engineering of Agricultural Machinery from Tehran University. His field of research is Machine vision and Post-harvest. **B. Mohammadi Alasti** obtained his PhD in Mechanical Engineering of Agricultural Machinery from the Islamic Azad University, Science and Research Branch, Tehran, Iran. His field of research is MEMS and NEMS.

---

## 1 INTRODUCTION

---

The term “combination” means blending and mixing, and it technically refers to a machine that performs multiple agricultural practices at the same time. Using functionality of different tools (e.g. moldboard plow, disk, leveler, seeder, roller, etc.) gathered together in a single set and in form of a machine leads to a device called combination (combined machine). This machine is capable of performing different tasks (including bed preparation, planting, leveling, and soil fixation) in just one pass on the field. The emergence of such a collection bring about accelerated work, timely practices, and also cost, time and energy efficiency. Moreover, reduction in tractor and machinery passes on the field can prevent the formation of hardpans. Recently, with regard to the mechanization sector’s demand, importing and manufacturing of combinations were increased, and they became more prevalent. These systems were used for planting seeds ranging between 2 and 10mm and for seed drilling. Two types of furrow opener are common in combination systems: disk furrow opener capable of performing in fields covered with plant residues (such as corn) and in high moisture content soils, as well as exactly adjusting the depth; and shoe furrow opener which has low wear (dry) and is suitable for properly loosened fields.

No-till machinery should be capable of cutting through unplowed soil and passing planting residues through furrow opener hitch links, and also providing a proper contact between soil and seeds [1]. Moreover, the type of residues, their density per area unit, and how well they are chopped are among the important factors effective in designing direct planting machinery. Research shows that the best arrangement for passing plant residues beneath a planter is when they are left upright on the ground. Chopped residues can, on the one hand, be accumulated in front of machinery hitch links and, on the other hand, disrupt the soil-seed contact [2]. The maximum penetration in hard and dry soils can be provided using shovel type furrow openers. However, these can disrupt the surface soil layer and mix plant residues with this layer [3]. With worldwide increasing demand for no-till machinery, disk furrow openers became of great interest since they disrupt only a small portion of soil volume. This characteristic minimizes the germination of weed seeds and maintains soil moisture. Their other significant characteristics include their suitability for high-speed planting (i.e. low soil throwing) and their ability to pass over plant residues without accumulating them in front of the hitch links. Disk furrow openers are made and used in various forms. The main criteria in designing a direct planter with disk furrow openers are shape selection, their arrangement, and their combination

with regard to soil conditions and planting pattern [4]. Traveling speed is also another factor contributing to the performance of furrow openers. Generally, the wider the furrow opener, the more effective the traveling speed will be in its performance [5]. The amount of pressure on each opener is yet another important factor in designing direct planters with disk furrow openers. The first difference between a planter used in conventional tillage practices and the one used in a no-till practice can be their weight. Since openers used in no-till conservative practices must cut through unplowed soils and plant residues, more pressure is required to drive them into soil. This lead to machinery overweight, especially in hard soils covered with wooden residues [6]. An effective approach to curbing machinery overweight is to use active furrow openers, which can facilitate cutting with their proper rotational movement along the traveling direction.

In arid and semi-arid areas of Iran, the high evaporation between harvesting and next planting stages and also the lack of organic matters at soil’s surface layer can harden the area’s structure less soil to the extent that, unless the plow practice is performed, furrow openers of grain drills and even the tough arms of deep drills will fail to penetrate. Against this background, most research efforts on no-till systems have used grain drills that had opener penetration issues or had to impose high pressure on machinery arms which, in turn, produced a plowed surface layer. Therefore, mixed results are reported in these studies, making it hard to draw a single conclusion.

The current study builds on the results from research efforts on no-till machinery in arid and semi-arid areas. These studies have frequently reported penetration issues which have led to crushing and bending of machinery due to impose high pressures on the opener unit and its collision with rocks and gravels. Therefore, with regards to the observed disfigurements and damages to furrow openers, Solid Works and ANSYS were employed to optimally design and analyze the components of a furrow opener. At the first design stage, a general view of the furrow opener unit of no-till machinery was required, which was provided by a visual examination. It was essential to prepare separate drawings for its components. To this effect, drawing on the inverse engineering concept, all components were dismantled and analysed.

---

## 2 MATERIALS AND METHODS

---

The optimal design of the furrow opener was performed by building on the soil properties from fields of arid and semi-arid areas and also the results from studies on no-till machineries working on such fields. The ASAE standard table was the reference for design

calculations. Then, Solid Works was used for the simulation process. ANSYS and the finite element method were employed for analyzing the furrow opener components.

**2.1 MODELING OF FURROW OPENER SET**

A 3D model of the furrow opener set in a Bertini no-till machine was designed and modelled in Solid Works (Fig. 1). The technical specifications are presented in Table 1.

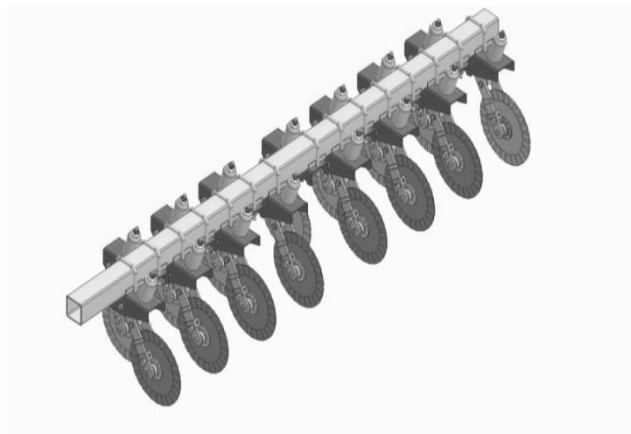


**Fig. 1** 3D model of the furrow opener

**Table 1.** The technical specifications

Characteristic	Value
Work width	300cm
Spacing and the number of units in line planting	17.5cm
Spacing and the number of units in row planting	35cm
Depth of planting	1-7cm
Machine's weight	3400kg
Required force	67kW
Opener's diameter	40cm
Opener's hitch link length	90cm
Total width	430cm

**2.1.1 OPTIMAL DESIGN AND MODELING OF OPENER'S COMPONENTS**

The furrow opener set of a no-till machine includes a number of opener units. Each unit consisted of a disk coultter, hub, bushing, hitch link, secondary chassis, main chassis, and safety spring. The main components are depicted in Fig. 2 to Fig. 5.

Cutting Unit:

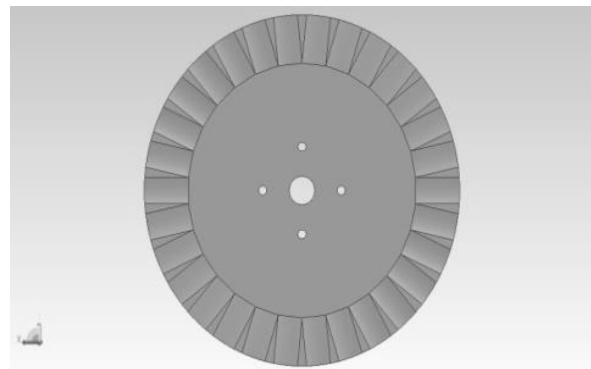


**Fig. 2** Disk-type furrow opener

Furrow Opener's Hub:

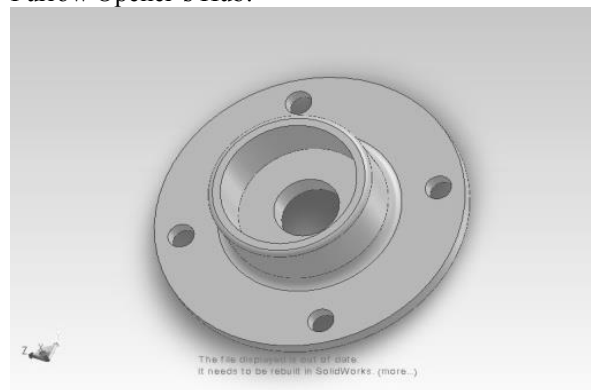


**Fig. 3** Furrow opener's hub

Pivot Bushing of Furrow Opener's Frame:

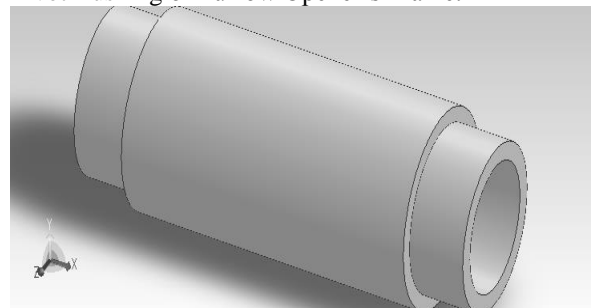


**Fig. 4** Furrow opener's bushing

Furrow Opener's Hitch Link:

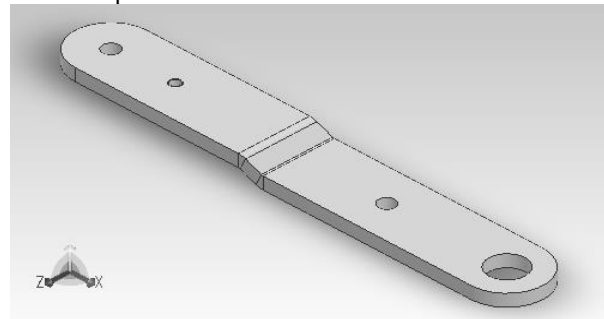


**Fig. 5** Furrow opener's hitch link

**Table 2** The mechanical properties of materials used for each unit's components

Materials	Density (kgm <sup>-3</sup> )	Final strength/ Tension- pressure (Pa)	Yield strength/ Tension- pressure (Pa)	Young's modulus (Pa)	Thermal expansion coefficient (Jkg <sup>-1</sup> )
Steel (ASTM-A37)	7850	4.6x10 <sup>8</sup>	2.5x10 <sup>8</sup>	2 x10 <sup>8</sup>	434

ASTM-A37 steel was selected for these components with regards to the imposed loads. The mechanical properties of this steel are presented in Table 2.

## 2.2 FORCES IMPOSED ON THE OPENER UNIT

### 2.2.1 FORCES ON THE ROTARY COULTER (DISK-TYPE FURROW OPENER)

The free body diagram of a rotary coultter is as follows: According to Fig. 6, the equivalent force imposed by soil on the  $\widehat{CD}$  arc due to the forward movement of the coultter is supposed as  $K_n$ . This force is acting at the middle of the  $\widehat{CD}$  arc.

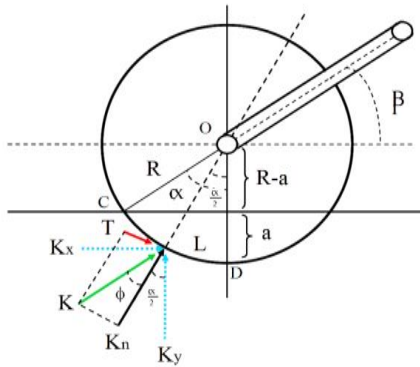


**Fig. 6** The free body diagram of a rotary coultter

It can be determined using the following equation:

$$K_n = K_0 L = K_0 (R\alpha) \quad (1)$$

Where,  $K_n$  is the force acting on the coultter from soil (N),  $K_0$  denotes the soil rigidity coefficient (N/m),  $L$  is the length of the  $\widehat{CD}$  arc (m),  $R$  is the radius of the coultter (m), and  $\alpha$  is the central angle of the  $\widehat{CD}$  arc in degrees. Moreover,  $\beta$  is the angle between the coultter's hitch link and the horizontal line. On the other hand, the total force,  $\vec{K}$ , can be obtained from the summation of the equivalent vector force,  $\vec{K}_n$ , and the tangent force between the coultter and soil,  $\vec{T}$ , as follows:

$$\vec{K} = \vec{K}_n + \vec{T} \quad (2)$$

The total force,  $\vec{K}$ , is determined using Equation 3:

$$K = \frac{K_n}{\cos \varphi} \quad (3)$$

Where,  $\varphi$  is the angle between  $K$  and  $K_n$ , which according to standards in Table 3, is the friction between soil and the coultter's steel. In order to determine the tangent force of the coultter, the following equations are used [7]:

$$T = K_n \tan \varphi \quad (4)$$

Furthermore,  $\alpha$  is determined as follows:

$$\alpha = \cos^{-1} \frac{R-a}{R} \quad (5)$$

As a result,  $\alpha$  is equal to 70.51 degrees. The total force ( $K$ ) was resolved into its vertical and horizontal components. In order to determine the tension on the coultter, Equation 6 was employed:

$$D = F_i [A + B(S) + C(S)^2] WT \quad (6)$$

Where,  $D = K_x$  is the force imposed on instruments (N),  $F$  is determined using the standard table for designing a furrow opener (3) in Appendix, and it shows the soil texture type, according to Table 3,  $I$  is specific soil parameters, in which -1 is used for light texture soils, -2 for medium texture soils, and -3 is for heavy texture soils.  $A$ ,  $B$  and  $C$  are implement-specific parameters in Table 3. Moreover,  $S$  is the forward speed (km/h),  $w$  is the machine width with the number of rows or planting units,  $T$  denotes the tillage depth which, for main tillage implements, is in centimeter (cm) and, for planter cutters, is a dimensionless quantity and equal to 1. The parameters associated with draft and preferred draft range (for tillage and planting implements) are estimated using Table 3. With regards to machine specifications, the coultter row under Seeding Implements and Grain Drill No-Till topics was

selected and the related quantities were used for the following equation:]

$$D = 1 \times [720 + 0 + 0] \times 1 \times 1 = 720 \text{ N} \tag{7}$$

Note that the coulter is capable of bearing up to 972N with a 4mm thickness:

$$D_{\text{Final}} = 720 + (0.35 \times 720) = 972 \text{ N} \tag{8}$$

The maximum force for the 4mm coulter was 972N. The unknown parameters of the above equations were calculated using Table 3. Then, the design was proceeded for a 6mm coulter, and its related  $K_x$  and  $K_y$  during a tillage operation were determined. Its results were compared to those from the 4mm coulter.

$$K_x = k \sin\left(\frac{\alpha}{2} + \varphi\right) \xrightarrow{\text{yields}} k = 981 \text{ N}$$

$$K_y = k \cos\left(\frac{\alpha}{2} + \varphi\right) \xrightarrow{\text{yields}} K_y = 119.87 + 734.6 = 854.471 \text{ N} \tag{9}$$

Therefore, compressive stresses on the coulter's section ( $\hat{CD}$ ) can be obtained from Eq. (10).

$$\sigma = \frac{K_n}{A} \tag{10}$$

Where,  $\sigma$  is the compressive stress (N/m<sup>2</sup>), and the involved section of the coulter is in m<sup>2</sup>.

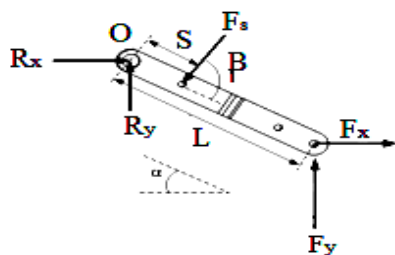


Fig. 7 Free body diagram of forces acting on the hitch link

### 2.2.2 FORCES ACTING ON HITCH LINK

In order to design a coulter, it is first necessary to calculate the draft imposed on its components when it engages the soil. Therefore, using Table 3, the draft was estimated. The following free body diagram presents the forces acting on a coulter's hitch link in no-till implements (Fig. 7). Eq. (9) can be used to determine the draft on a coulter's hitch link in no-till implements. The force,  $F_s$ , can be obtain using the following relation:

$$\begin{cases} \sum M_o = 0 \\ F_s S \sin \beta - F_y L \cos \alpha - F_x L \sin \alpha = 0 \end{cases} \tag{11}$$

### 2.2.3 FORCES ACTING ON COULTER'S HUB

The numerical calculations of the forces on the hub along the x and y axes (as shown in Fig. 8) were performed using Eq. (9).

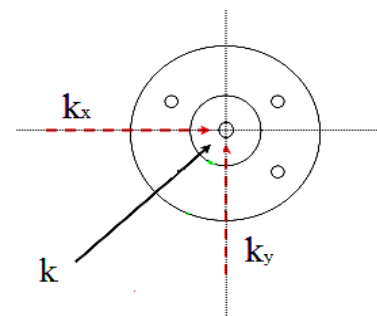


Fig. 8 Forces acting on the coulter's hub

Equation 9 was also used to determine the equivalent force of the hub along the x and y axes. Therefore, the resultant vector from the addition of the said forces, the equivalent force,  $K$ , of 981N was obtained.

### 2.2.4 FORCES ACTING ON THE COULTER'S BUSHING

Eq. (9) was also used to determine the bushing's forces along the x and y axes. The equivalent force,  $K$ , was 981N. This amount was divided into two at both ends of the bushing.

### 2.3 SAFETY FACTOR

The von Mises theory was used for this purpose. According to the theory, the maximum stress on an object can be determined using the following relation:

$$\left[ \sigma_{\text{max}} = \frac{(\sigma_1 - \sigma_2)^2 + (\sigma_2 - \sigma_3)^2 + (\sigma_1 - \sigma_3)^2}{2} \right]^{1/2} \tag{12}$$

Where,  $\sigma_1$ ,  $\sigma_2$  and  $\sigma_3$  are the main stresses acting on an object along three coordinate axes. In order to ensure the performance of mechanical materials and to prevent failure, the applied stresses on an object should be smaller than its yield stress. According to this principle,

the safety factor of an object can be determined as follows:

$$F.S = \frac{\sigma_y}{\sigma_{max}} \tag{13}$$

All parameters in the above relation are in Newton. Once the design calculations of the coulters were checked with table 3, it was found that the actual forces are multiple times larger than in the theory. Empirically and practically, coulters sustain heavy damages during operation. Due to unknown environmental factors in soil, existence of fine and coarse gravels, and also different partial, unpredictable loads produced on impact with the soil, it was concluded that the coulters' thickness must be increased. On the other hand, there are numerous factors acting on soil; therefore, the safety factor was also increased. To design these four components,  $K_x = 981N$  and  $K_y = 854.47N$  were obtained.

**2.4 MESHING AND LOADING FOR MAIN COMPONENTS OF THE COULTER**

In the optimal designing of a coulters and its main involved components, the static loading approach was used. Element type was triangular. The finer the meshing, the more accurate the analysis. Fig. 9 to Fig. 15 show the meshing and loading processes of the main coulters components; where A, B and C specify the backrest, displacement and the applied force.

Coulters Meshing:

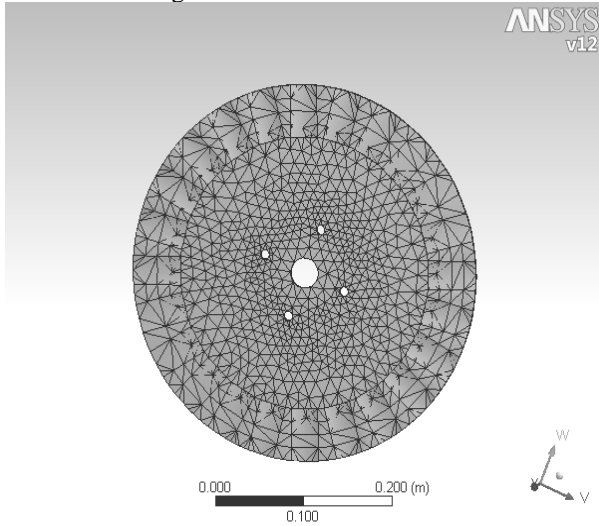


Fig. 9 Triangular meshing of the disk-type furrow opener

Coulters Loading:

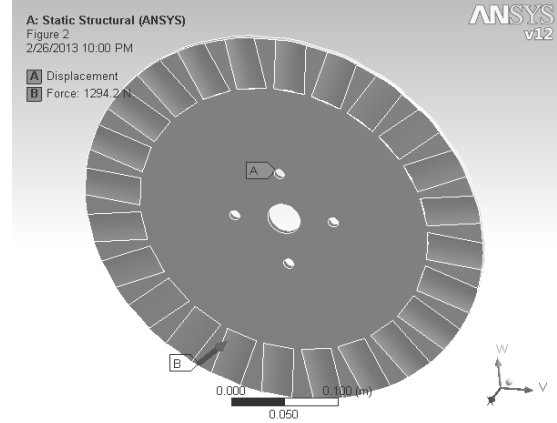


Fig. 10 (A): force applied to furrow opener, (B): backrest displacement

Hub Meshing:

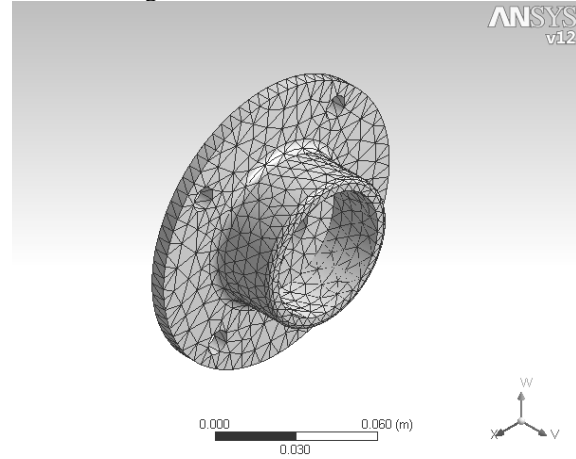


Fig. 11 Triangular meshing of the coulters hub

Hub Loading and Backrest:

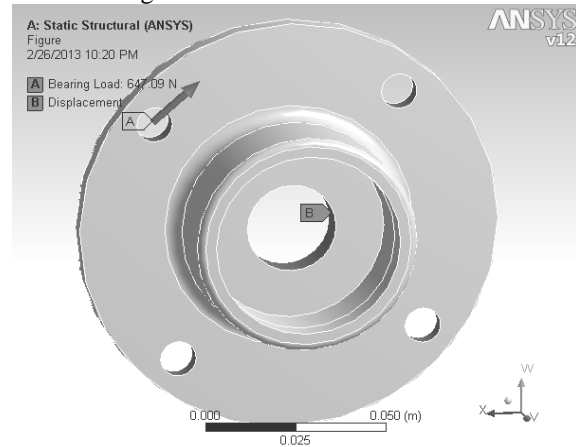


Fig. 12 Furrow opener's hub loading and backrest

Hitch Link Meshing:

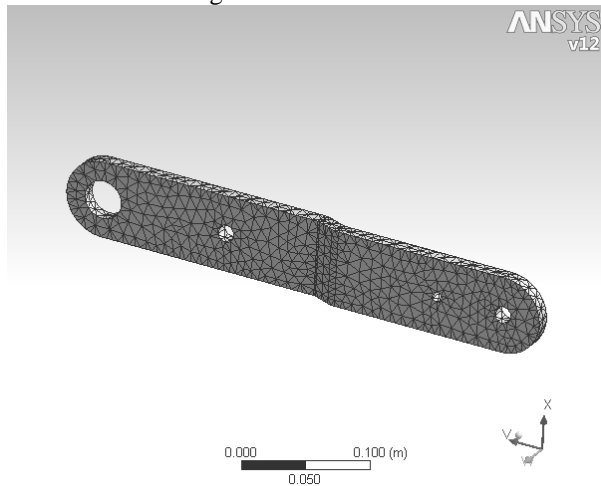


Fig. 13 Triangular meshing of the couler's hitch link

Bushing Loading and Backrest:

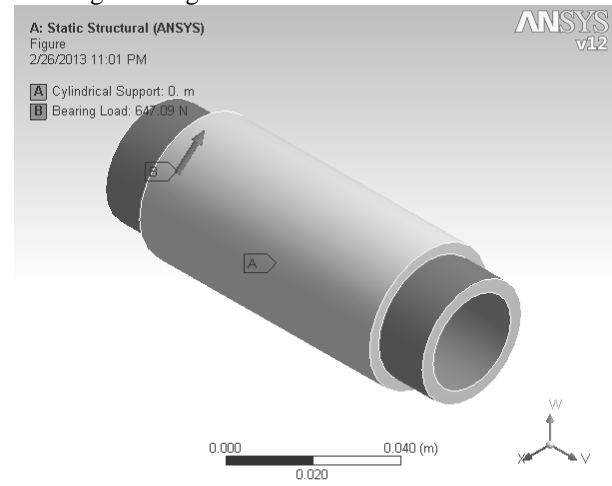


Fig. 16 Couler's bushing loading and backrest

Hitch Link Loading:

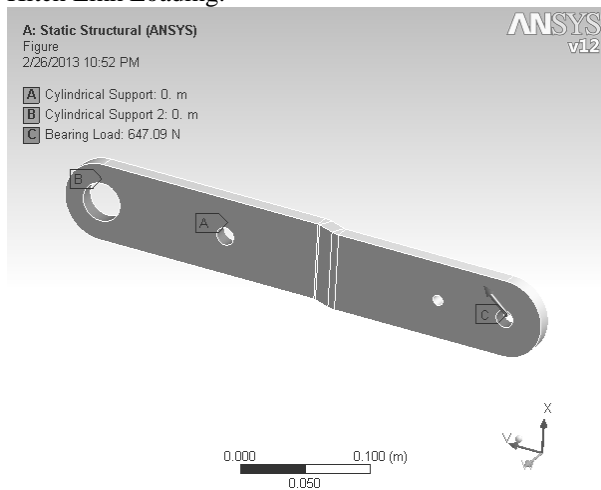


Fig. 14 Furrow opener's hitch link loading and backrest

Bushing Meshing:

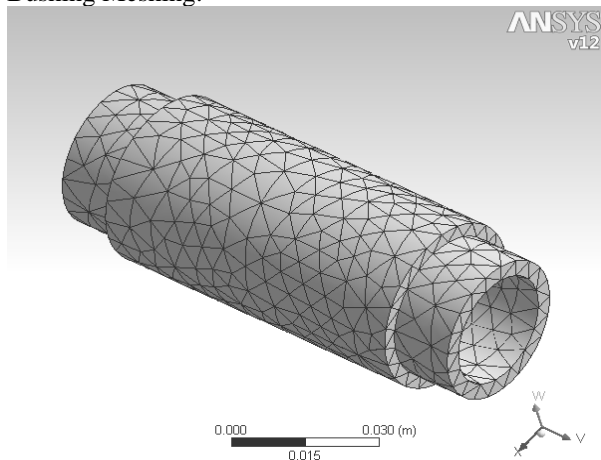


Fig. 15 Triangular meshing of the couler's bushing

### 3 RESULTS AND DISCUSSIONS

The maximum force that can be borne by the couler of the no-till implement with a 4mm diameter was 972N. Given  $\phi = 47.726$ , the value of  $K_y$  was 854.471N. Moreover,  $K_x$  was 981N. The maximum tension that the optimal couler can hold along the horizontal axis was 981N.

#### 3.1 STRESS ANALYSIS OF THE 4MM COULER (VON MISES THEORY)

According to the stress analysis of the couler shown in Fig. 17, the minimum stress of the couler was 2124.7 Pa at most points on the plane, while its maximum occurred at both its impact point with soil and a part of its backrest was  $1.4133 \times 10^7$  Pa.

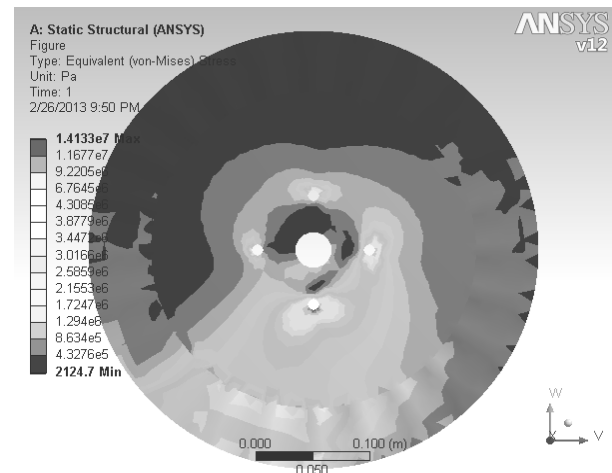


Fig. 17 Stress of a couler with a 4mm diameter

### 3.1.1 STRESS ANALYSIS OF THE OPTIMAL COULTER WITH A 6MM DIAMETER

According to the stress analysis of the coultter shown in Fig. 18 (based on the von Mises criterion), the minimum stress of the coultter throughout the plane was 1985.5 Pa, while its maximum was occurred at holes used for connecting to the hub with  $1.0829 \times 10^7$  Pa.

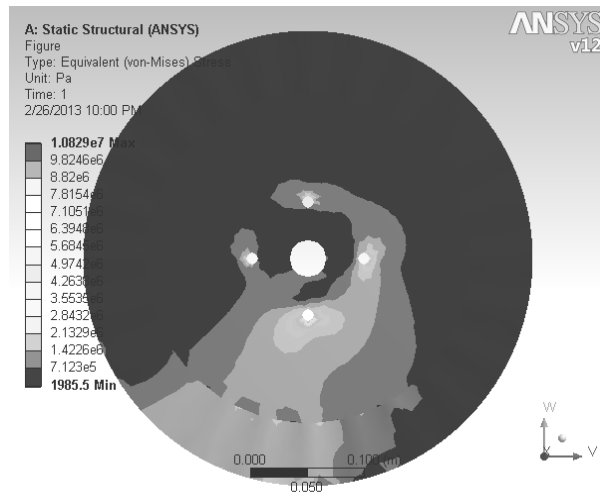


Fig. 18 Optimal coultter stress with a 6mm diameter

### 3.3 DEFLECTION ANALYSIS IN THE 6MM OPTIMAL COULTER

According to Fig. 20, the applied forces during the implement's forward movement cause deflection in the optimal coultter, as its maximum ( $3.128 \times 10^{-6}$  m) occurred at the edge engaged with soil. However, no deflection was observed at the central areas of the plate.

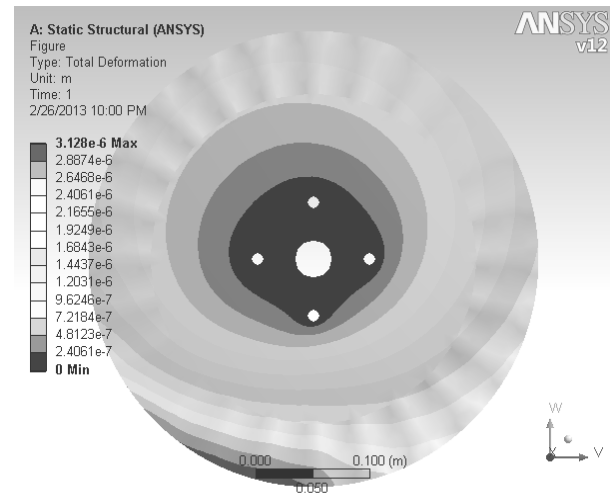


Fig. 20 Deflection in the 6mm coultter

### 3.2 RESULTS FROM DEFLECTION ANALYSIS OF THE 4MM COULTER

As shown in Fig. 19, the applied forces during the implement's forward movement cause deflection in the coultter, as its maximum ( $5.628 \times 10^{-6}$  m) occurred at the edge engaged with soil. However, no deflection was observed at the central areas of the plate.

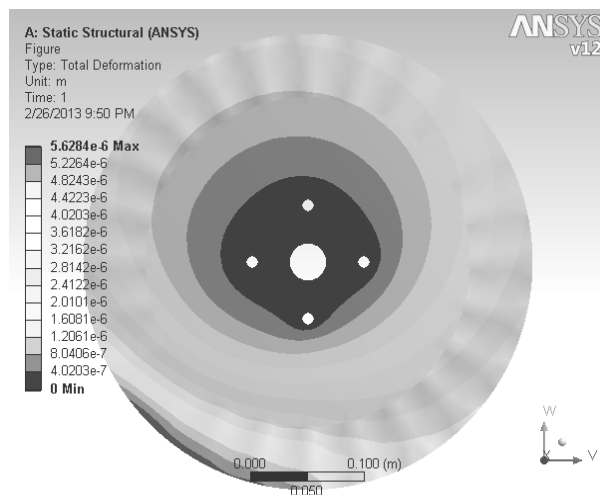


Fig. 19 Deflection in the 4mm coultter

### 3.4 RESULTS FROM STRESS ANALYSIS OF HUB

Using the von Mises criterion, the stress analysis of the hub shown in Fig. 21 indicated that the minimum stress of the hub was 4228.1 Pa throughout the plane except around the holes, while its maximum was inside the hub's holes with  $5.7744 \times 10^6$  Pa.

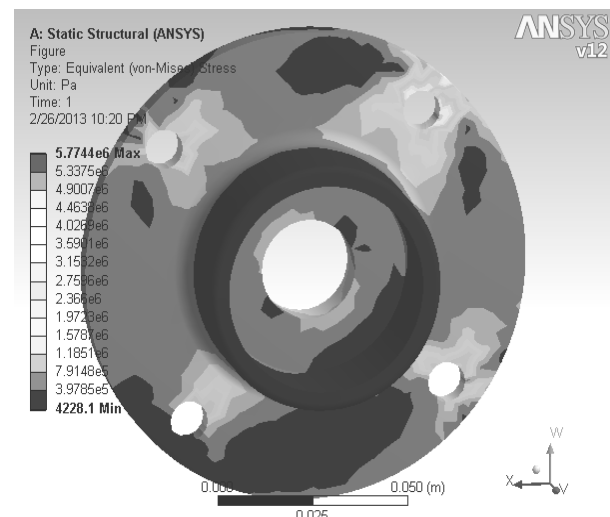


Fig. 21 Stress analysis of the coultter's hub



### 3.4.1 RESULTS FROM DEFLECTION ANALYSIS OF THE HUB

As shown in Fig. 22, the maximum deflection of the coulters hub ( $5.4784 \times 10^{-7}$  m) occurred when forces acted on the hub's center along the implement's movement direction. This is while its minimum (zero) was observed around the bolt holes.

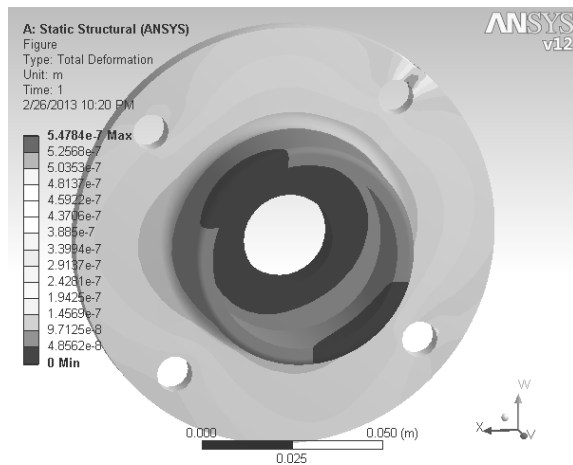


Fig. 22 Deflection analysis of the coulters hub

### 3.5.1 RESULTS FROM DEFLECTION ANALYSIS OF HITCH LINK

As shown in Fig. 24, the maximum deflection of the hitch link ( $5.3903 \times 10^{-5}$  m) occurred at its point of connection to the coulters due to forces along the implement's movement direction. This is while its minimum was observed at the backrest and its close vicinity with  $1.0168 \times 10^{-7}$  m.

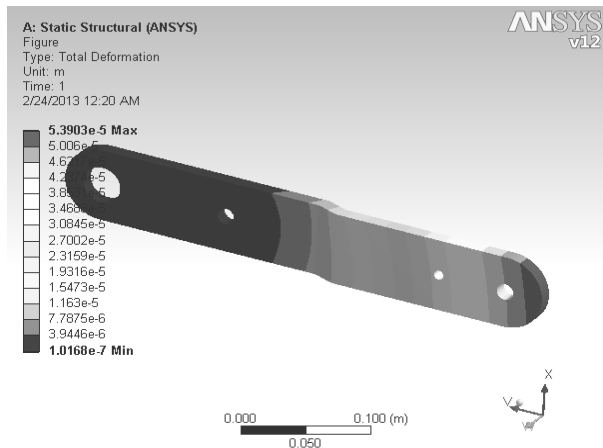


Fig. 24 Deflection in the coulters hitch link

### 3.5 RESULTS FROM STRESS ANALYSIS OF HITCH LINK

Using the von Mises criterion, the stress analysis of the hitch link shown in Fig. 23 indicated that the minimum stress of the hitch link was 3151.3 Pa at its both ends, while its maximum was at the middle of the hitch link and along the instrument traveling direction with  $2.4719 \times 10^7$  Pa.

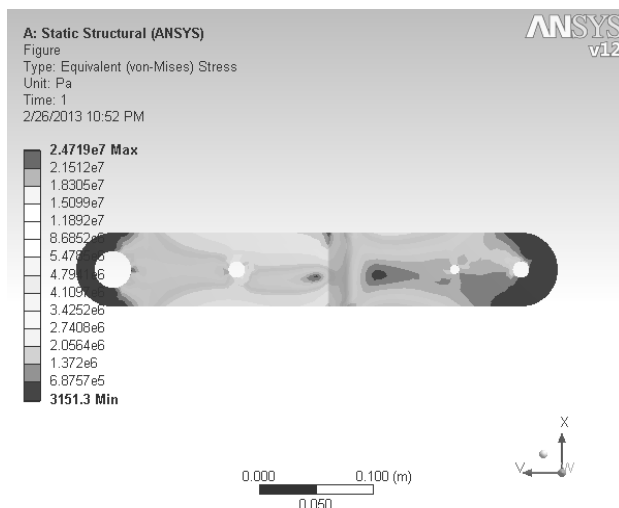


Fig. 23 Stress in the coulters hitch link.

### 3.6 RESULTS FROM STRESS ANALYSIS OF FRAMES PIVOT BUSHING

According to Fig. 25, the stress analysis for the frame's joint bushing indicated that the minimum stress in this component was at its middle with 32.806 Pa and the maximum stress was observed at its both ends with  $9.618 \times 10^5$  Pa.

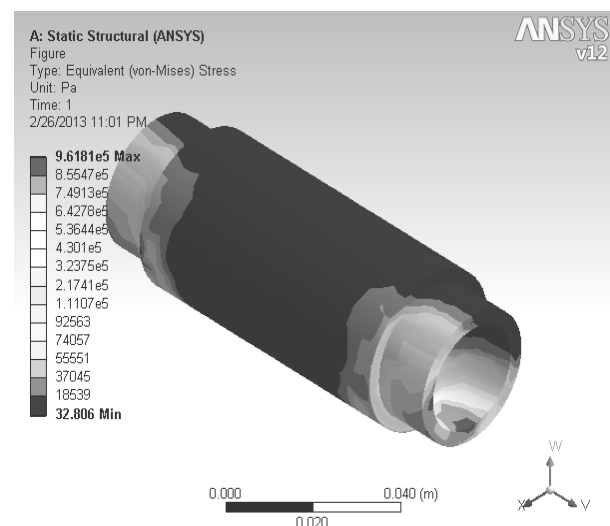


Fig. 25 Stress in the coulters bushing

### 3.6.1 DEFLECTION IN THE FRAME'S JOINT BUSHING

As shown in Fig. 26, forces applied to the implement along its movement direction produced deformations in the frame's joint bushing. The maximum deflection was  $1.4211 \times 10^{-8}$  m at the point where the force was applied, and the minimum was around zero at other parts of the bushing.

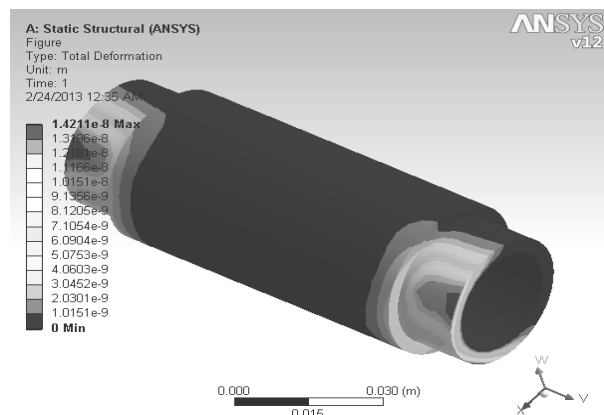


Fig. 26 Deflection analysis of the coulter's bushing

## 4 CONCLUSION

With regards to Table 3 in the Appendix, the maximum tension that can be borne by the coulter was 720N. Given a 35% correction factor in Table 3 for designing, the coulter's maximum tension can be increased to 972N. However, in practice, the applied forces are multiple times larger than in theory. Empirically and practically, coulters sustain heavy damages during operation. The coulter's stress can be reduced and its strength and safety factor can be boosted by optimally designing the components of a furrow opener.

Note that the alloy used for the share was regular iron ( $2.5 \times 10^8$  Pa) and the share's thickness was increased. The maximum stress of the optimal 6mm coulter was  $1.0829 \times 10^7$  Pa. The maximum bearable stress by the 4mm coulter was  $1.4133 \times 10^7$  Pa. The maximum deflection of the optimal 6mm coulter was  $3.128 \times 10^{-6}$  m which was smaller than the deflection in the 4mm coulter ( $5.628 \times 10^{-6}$  m). The safety factor of the 4mm coulter was 17.85 while it was increased to 25 in the 6mm coulter.

Finally, the results showed that the optimal furrow opener is durable and will not face deformation under applied forces. It is also more cost-effective. Under loading conditions, the maximum stress along the

implement forward movement occurred in the hub's holes with  $5.7744 \times 10^6$  Pa.

By optimally designing the coulter's hitch link, the stress concentration area is widened. The maximum stress concentration was also occurred in the drawbar's bolt holes. From an economical point of view, the 10mm bolts in the hitch link were replaced by 12mm bolts. Note that the maximum stress at the front side of the hitch link and along the instrument movement direction was  $2.4719 \times 10^7$  Pa.

In the optimally designed frame's joint bushing, the strength was boosted while stress and deflection were mitigated. The maximum stress was recorded at both ends of the bushing with  $9.618 \times 10^5$  Pa, while the minimum amount with 32.806 Pa occurred at its middle point when applied forces were along the instrument movement direction.

## REFERENCES

- [1] Cannell, R., Ellis, F., Christian, D., Graham, J., and Douglas, J., "The Growth and Yield of Winter Cereals After Direct Drilling, Shallow Cultivation and Ploughing on Non-Calcareous Clay Soils", *The Journal of Agricultural Science*, Vol. 94, No. 2, 1980, pp. 345-359.
- [2] Hemmat, A., Taki, O., "Grain Yield of Irrigated Winter Wheat as Affected by Stubble-Tillage Management and Seeding Rates in Central Iran", *Soil and Tillage Research*, Vol. 63, No. 1, 2001, pp. 57-64.
- [3] Hofman, V., Fanning, C., and Deibert, E., "Reduced Tillage Seeding Equipment for Small Grains", 2011.
- [4] Stephens, L., Johnson, R., "Soil Strength in the Seed Zone of Several Planting Systems", *Soil Science Society of America Journal*, Vol. 57, No. 2, 1993, pp. 481-489.
- [5] Goshtasb, A. K., Desbiolles, J., and Fielke, J., "Circular Disc Blade Considerations in Soil Force Prediction Modelling", *Journal of Agricultural Science and Technology A*, Vol. 4, No. A, 2014.
- [6] Boone, L., Graffis, D., Gray, M., Hager, A., Hoeft, R., and Hollinger, S., "Illinois Agronomy Handbook", University of Illinois at Urbana-Champaign, Agricultural Experiment Station, USA, 1994.
- [7] Mashaly, M., El-Shafiy, H., El-Maraghy, S. and Habib, H., "Synthesis, Properties and Thermal Studies of Oxorhenium (V) Complexes with 3-Hydrazino-5, 6-Diphenyl-1, 2, 4-Triazine, Benzimidazolethione and 2-Hydrazinobenzimidazole: Mixed Ligand Complexes, Pyrolytical Products and Biological Activity", *Spectrochimica Acta Part A: Molecular and Biomolecular Spectroscopy*, Vol. 61, No. 8, 2005, pp. 1853-1869.

Appendix Table 3 ASAE Standard Parameters for Designing Furrow Openers

Implement	SI Units				English Units				Soil Parameters			Range + %
	Width Units	Machine Parameters			Width Units	Machine Parameters			F <sub>1</sub>	F <sub>2</sub>	F <sub>3</sub>	
		A	B	C		A	B	C				
<b>MAJOR TILLAGE TOOLS</b>												
Subsolder/manure injector												
Narrow point	tools	226	0.0	1.8	Tools	129	0.0	2.7	1.0	0.70	0.45	50
30 cm winged point	tools	294	0.0	2.4	Tools	167	0.0	3.5	1.0	0.70	0.45	50
Moldboard plow	m	652	0.0	5.1	n	113	0.0	2.3	1.0	0.70	0.45	40
Chisel plow												
5 cm straight point	tools	91	5.4	0.0	Tools	52	4.9	0.0	1.0	0.85	0.65	50
7.5 cm shov / 35 cm sweep	tools	107	6.3	0.0	Tools	61	5.8	0.0	1.0	0.85	0.65	50
10 cm twisted shovel	tools	123	7.3	0.0	Tools	70	6.7	0.0	1.0	0.85	0.65	50
Sweep plow												
Primary tillage	m	390	19.0	0.0	n	68	5.2	0.0	1.0	0.85	0.65	45
Secondary tillage	m	273	13.3	0.0	n	48	3.7	0.0	1.0	0.85	0.65	35
Disk harrow, tandem												
Primary tillage	m	309	16.0	0.0	n	53	4.6	0.0	1.0	0.88	0.78	50
Secondary tillage	m	216	11.2	0.0	n	37	3.2	0.0	1.0	0.88	0.78	30
Disk gang, Single												
Primary tillage	m	124	6.4	0.0	n	21	1.8	0.0	1.0	0.88	0.78	25
Secondary tillage	m	86	4.5	0.0	n	15	1.3	0.0	1.0	0.88	0.78	20
Counters												
Smooth or ripple	tools	55	2.7	0.0	Tools	31	2.5	0.0	1.0	0.88	0.78	25
Bubble or bube	tools	66	3.3	0.0	Tools	37	3.0	0.0	1.0	0.88	0.78	25
Field cultivator												
Primary tillage	tools	46	2.8	0.0	Tools	26	2.5	0.0	1.0	0.85	0.65	30
Secondary tillage	tools	32	1.9	0.0	Tools	19	1.8	0.0	1.0	0.85	0.65	25
Row crop cultivator												
s-line	rows	140	7.0	0.0	rows	80	6.4	0.0	1.0	0.85	0.65	15
c-shank	rows	260	13.0	0.0	rows	148	11.9	0.0	1.0	0.85	0.65	15
No-till	rows	435	21.8	0.0	rows	248	19.9	0.0	1.0	0.85	0.65	20
Rod weeder	m	210	10.7	0.0	n	37	3.0	0.0	1.0	0.85	0.65	25
Disk bedder	rows	185	9.5	0.0	rows	106	8.7	0.0	1.0	0.88	0.78	40
Minor tillage tools												
Rotary hoe	m	600	0.0	0.0	n	41	0.0	0.0	1.0	1.0	1.0	30
Coil tine harrow	m	250	0.0	0.0	n	17	0.0	0.0	1.0	1.0	1.0	20
Spike tooth harrow	m	600	0.0	0.0	n	40	0.0	0.0	1.0	1.0	1.0	30
Spring tooth harrow	m	2.000	0.0	0.0	n	135	0.0	0.0	1.0	1.0	1.0	35
Roller packer	m	600	0.0	0.0	n	40	0.0	0.0	1.0	1.0	1.0	50
Roller harrow	m	2.600	0.0	0.0	n	180	0.0	0.0	1.0	1.0	1.0	50
Land plane	m	8.000	0.0	0.0	n	550	0.0	0.0	1.0	1.0	1.0	45
Seeding implements												
Row crop planter, prepared seedbed mounted												
Seeding only	rows	500	0.0	0.0	rows	110	0.0	0.0	1.0	1.0	1.0	25
Drawn												
Seeding only	rows	900	0.0	0.0	rows	200	0.0	0.0	1.0	1.0	1.0	25
Seed, fertlizer, herbicides	rows	1.550	0.0	0.0	rows	350	0.0	0.0	1.0	1.0	1.0	25
Row crop planter , no-till												
Seed, fertlizer, herbicides												
1	rows	1.820	0.0	0.0	rows	410	0.0	0.0	1.0	0.96	0.92	25
Row crop planter, zone-till												
Seed, fertlizer, herbicides												
3	rows	3400	0.0	0.0	rows	765	0.0	0.0	1.0	0.94	0.82	25
Grain Drill wipress wheels												
< 2.4 m drill width	rows	400	0.0	0.0	rows	90	0.0	0.0	1.0	1.0	1.0	25
2.4 to 3.7 m drill width	rows	300	0.0	0.0	rows	67	0.0	0.0	1.0	1.0	1.0	25
> 3.7 m drill width	rows	200	0.0	0.0	rows	25	0.0	1.0	1.0	1.0	1.0	25
Grain drill, no-til												
1	rows	720	0.0	0.0	rows	160	0.0	0.0	1.0	0.92	0.79	35
Hoe Drill	m	6100	0.0	0.0	n	420	0.0	0.0	1.0	1.0	1.0	50
Primary tillage	m	2900	0.0	0.0	n	200	0.0	0.0	1.0	1.0	1.0	50
Secondary tillage	m	3700	0.0	0.0	n	250	0.0	0.0	1.0	1.0	1.0	50
Pn Drill												